Scientific Journal of Silesian University of Technology. Series Transport
Zeszyty Naukowe Politechniki Śląskiej. Seria Transport

Volume 106 **2020**

p-ISSN: 0209-3324

e-ISSN: 2450-1549

DOI: https://doi.org/10.20858/sjsutst.2020.106.16

Journal homepage: http://sjsutst.polsl.pl

Article citation information:
Šulka, P., Sapietová, A., Bárnik, F. Vibrodiagnostics of rolling ball bearings connected with processing, result´s comparison and prediction of service life. *Scientific Journal of Silesian University of Technology. Series Transport*. 2020, **106**, 183-196. ISSN: 0209-3324. DOI: https://doi.org/10.20858/sjsutst.2020.106.16.

Peter ŠULKA[1], Alžbeta SAPIETOVÁ[2], František BÁRNIK[3]

VIBRODIAGNOSTICS OF ROLLING BALL BEARINGS CONNECTED WITH PROCESSING, RESULT´S COMPARISON AND PREDICTION OF SERVICE LIFE

Summary. This article deals with vibration analysis and the processing of the vibration signal obtained during the experimental measurement on a rotary shaft at start-up, constant speed and run-out, with rolling ball bearings. The next step of the research is the introduction and application of mathematical and numerical methods for the processing of input and measured data using diagnostic and mathematical software. The principle of measurement and processing was to compare the results of oscillation of an undamaged bearing with several types of damaged bearings with corresponding deformations in the orbits/raceways. The purpose of this research and comparison was to achieve optimal results (in terms of amplitude values, the occurrence of eigenvalue vibrations and the resonance phenomenon) of individual bearings with corresponding deformations in the raceways and to obtain calibration diagrams as a tool for possible prediction of bearings in operation.

Keywords: rolling ball bearing, vibrodiagnostics, evaluation, comparison

[1] Faculty of Mechanical Engineering, The University of Žilina, Univerzitná 8215/1, Žilina, Slovakia. Email: peter.sulka@fstroj.uniza.sk
[2] Faculty of Mechanical Engineering, The University of Žilina, Univerzitná 8215/1, Žilina, Slovakia. Email: alzbeta.sapietova@fstroj.uniza.sk
[3] Faculty of Mechanical Engineering, The University of Žilina, Univerzitná 8215/1, Žilina, Slovakia. Email: frantisek.barnik@fstroj.uniza.sk

1. INTRODUCTION

Measurement, data processing and mechanical vibration analysis are an integral part of the diagnostic system for monitoring the operating conditions of mechanical parts and machinery (roller ball bearing in our case) in every industry. The purpose and aim of diagnosing vibrations of machine components and machinery are to detect the occurrence and causes of the resonance phenomena, increased frequency amplitudes and noise of the machine component in service (rolling bearing) [4]. The next step in diagnosis is the possibility of eliminating the above-mentioned issues in order to ensure life prediction and maximise the safety and reliability of the mechanical component in operation [6,8,12].

2. MATHEMATICAL METHODS USED IN PROCESSING

Fourier transform and its applications together with wave transformations of various types are effective mathematical methods, which find effective use in processing and subsequent analysis of measured signals and data. Mathematical methods make it possible to obtain relevant results and information from measured data by applying generated algorithms of a given methodology using computer software. The output is a graphical representation of vibration signals in the time or frequency domain with the possible detection of adverse vibration phenomena [2,5,10].

2.1 Short-time Fourier transform (STFT)

The Short-term Fourier transformation is a time-frequency analytical tool for non-stationary signals. The transformation provides information about the signal f(t) and its spectrum F(ω) in the time-frequency window [2]. The principle of this method is to multiply the f(t) signal to be analysed by a certain type of symmetric window function (so-called window) ω*(t-τ) of constant length and then calculate the Fourier transform of the individual signal segments f). The STFT of the continuous signal f(t) is defined by the following formula (Equation 2) [6].

$$STFT\{x(t)\}(\tau,\omega) \equiv X(\tau,\omega) = \int_{-\infty}^{\infty} f(t)\omega * (t-\tau)\, e^{j\omega t} dt = < f(t).\omega * (t-\tau)e^{j\omega t} > \quad (1)$$

where the symbol (*) matches complex conjugation and t - time shift of the window. The most commonly used window elements are the Hamming, Kaiser, Gauss or Hann rectangular windows.

2.2 Fast Fourier transform (FFT)

Due to the fact that the calculation of the classical Fourier transform requires a considerable amount (N2), which is the most time-consuming operation, an algorithm was developed to allow a significant acceleration of the calculation [11]. This algorithm is described as FFT – Fast Fourier Transform (Equation 1).

$$X(k) = \sum_{i=0}^{N-1} x(i) \cdot l^{\frac{-j2\pi ik}{N}} = \sum_{i=0}^{N-1} x(i) cos\left(\frac{2\pi ik}{N}\right) - j \cdot \sum_{i=0}^{N-1} x(i) sin\left(\frac{2\pi ik}{N}\right) \quad (2)$$

The FFT algorithm uses the mathematical property of FT, which is the real output signal of the odd number of symmetric spectrum elements (Fig. 1) and complexly associated around its centre.

This means that the real component is around the centre even and the imaginary component is odd. As a result of this finding, it is enough to calculate the first half of the spectrum and the second will be identical to the opposite sign of the imaginary component [7].

2.3 Wavelet transform (WT)

The principle of Wavelet's transformation is to de-interleave and compose input signals through so-called functions wavelets. Essentially, the waves represent time-localised waves, respectively wave package. Wavelet transformation has all functions created from one basic function, called mother pattern. Prototype function of basic wavelength ψ(t) is generated by using two basic operations of scaling and time shifting [9].

$$WT_f(a,b) = \int_{-\infty}^{\infty} f(t)\ \psi^*_{[a,b]}(t)dt = \langle f(t),\ \psi_{[a,b]}(t)\rangle\ a \in R^+, b\ \in R \tag{3}$$

3. DESCRIPTION OF ANALYSED BALL BEARING

The aim of the analysis was to examine and analyse the oscillation of the investigated object, which was rolling ball bearing, is shown in Fig. 1. The mentioned ball bearing is connected to the rotary shaft in the test centre as can be seen in Fig. 2.

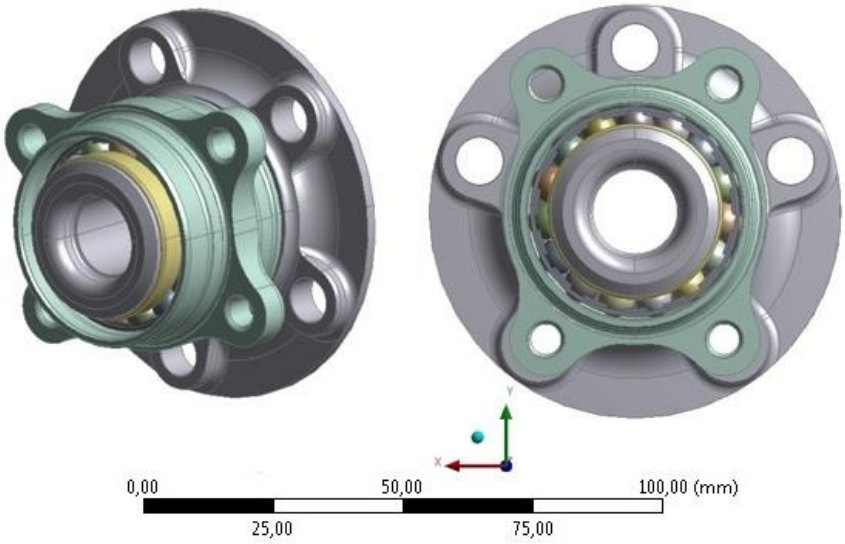

Fig. 1. 3D model of investigated rolling ball bearing

The measurement itself was carried out in several steps to examine and compare the individual bearings with respective deformations in the orbits. The basis of the measurement was to obtain data on the dynamic behaviour of individual bearings with and without deformations in orbits for the need to detect vibrations and to understand the behaviour of

the examined mechanical components during operation. Measurements were made at the start-up of the test device (with an appropriate bearing on the rotary shaft) at 1000 rpm, staying at this level of mentioned rpm and run-out of testing machinery in the cycle of approximately 50 s.

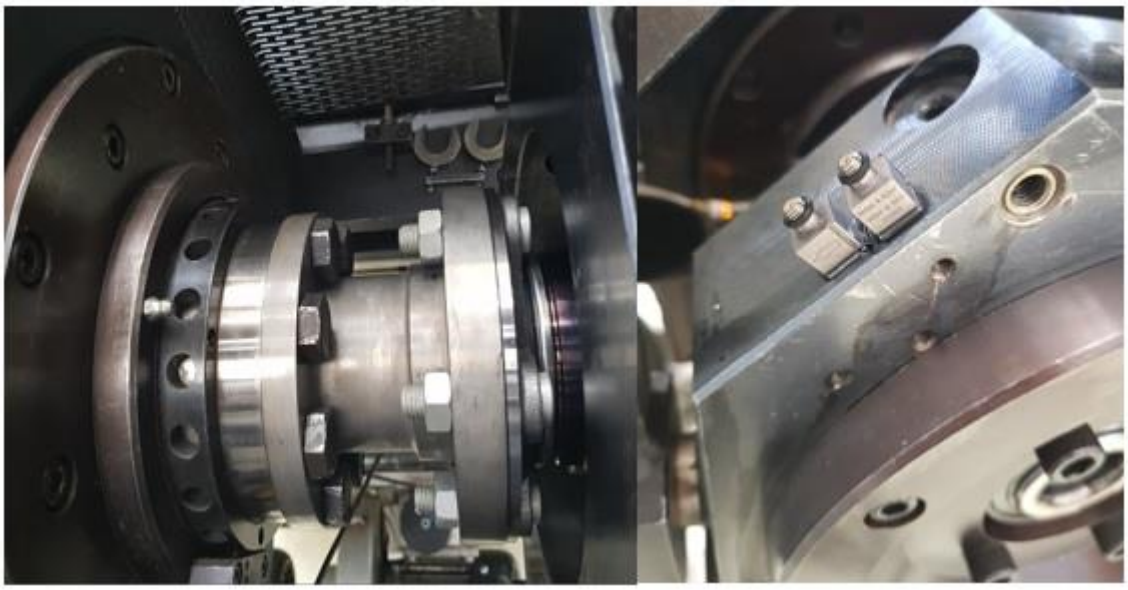

Fig. 2. The picture of mounted rolling ball bearing and sensors to the testing facility

The measurement process conditions were:

a) Installation of acceleration and measurement sensors.
b) Installation of individual bearings on the test facility.
c) Execution of measurements at specified time.
d) Measurement is always carried out on one bearing only.
e) The purpose to achieve the proposed maximum speed of 1000 rpm.
f) Compliance with the occupational safety protocol.

The essence of the measurement was to display the data and results used in the operating mode and to compare the results with the computational model (0 μm; 7.88955 μm; 48.7087 μm). The individual bearings were mounted together for acceleration (rotating shaft) and measurements were made on a test ramp of 1000 rpm, at constant speed and lowering for about 50 s, so that the radiation load of the bearings with a force of 40,495 N.

4. PROCESSING OF MEASURED DATA AND APPLICATION

Approximately 1,400,000 data representing acceleration values with a proposed sampling step of $3.9062525 \cdot 10^{-5}$ s were obtained by the process and measurement of individual bearings. The total measurement of each bearing was performed continuously for 50 s with a sampling frequency of 25,600 Hz, with the emphasis being placed on achieving a maximum speed of 1000 rpm, which corresponds to triggering of start-up, constant speed and run-out of testing machinery as shown in Fig. 3 (spectrum is equal for each bearing with given

deformation). The measurement itself took place in three different directions, namely in the radial, axial and tangential use of individual diagnostic sensors.

The obtained acceleration values were subsequently analysed using mathematical methods and mathematical software Diadem, LabView and Matlab R2019a.

For the overall analysis and diagnostics of individual bearing vibration, data corresponding to the axial direction of acceleration sensing were used, the reason being the most accurate results and graphical outputs in terms of comparison of the individual bearings with the corresponding indentation [1,3]. Another reason for using only axial direction data is that the bearing stiffness is lower in the axial direction than in the radial or tangential direction. For angular contact bearings, the resulting force component extends in both axial and radial directions. These facts show that the results from the axial scanning direction have the highest predictive value and thus provide the most accurate results of each simulation.

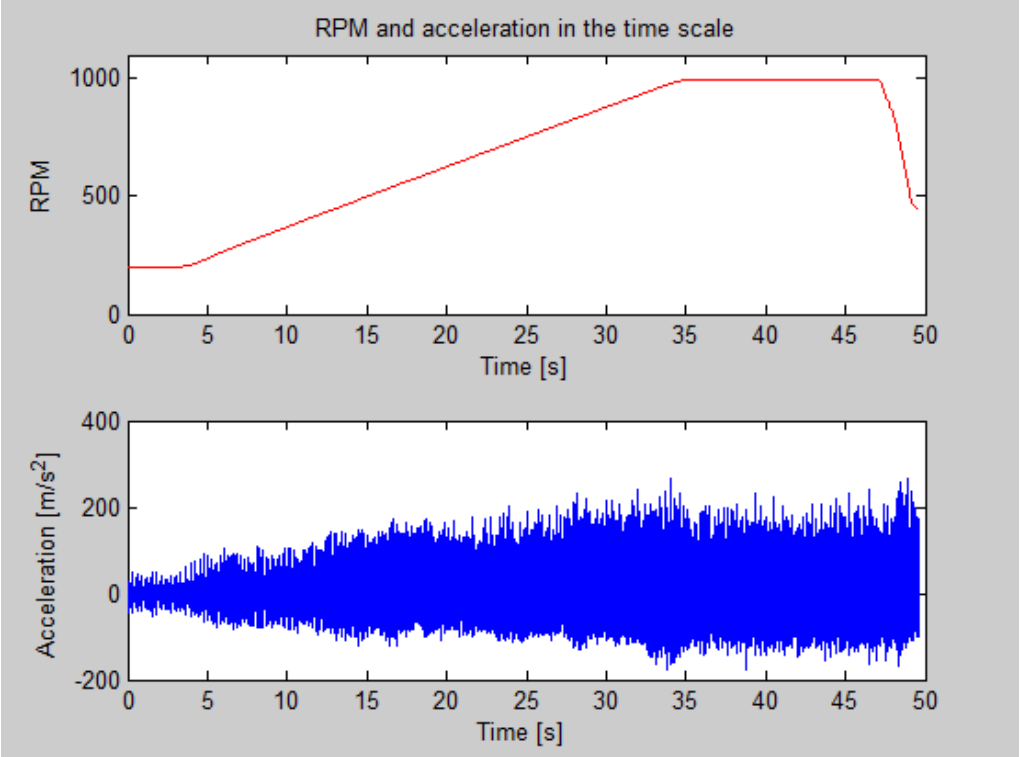

Fig. 3. Representation of measured speed [RPM] and acceleration [m/s^2] in the axial direction

5. TRANSFORMATION OF MEASURED DATA BY STFT

The short-term Fourier transform and the subsequent application of this mathematical theory serve as a tool to detect the adverse effects of vibration (increased vibration amplitudes, internal vibration patterns, resonance phenomenon, and increased noise). The most important advantage and characteristic of this mathematical method is the ability to detect adverse vibrations simultaneously in both time and frequency domains. An algorithm was developed and used in the Matlab R2019a software to diagnose vibrations and evaluate the results of the investigated deposits. The STFT (Spectrogram) algorithm gives us a graphical output in the form of a spectrogram (time-frequency vibration detection) and

a graphical representation of the projections of the individual time, frequency, and speed parameters plotted on the x-axis relative to the amplitude displayed on the y-axis. The STFT vibration treatment was performed for individual bearings with given orbital deformations. The graphical results for the 0 μm indented bearing are shown in Fig. 4, the 7.895 μm deformation is shown in Fig. 5 and the deformation 48.7087 μm is shown in Fig. 6.

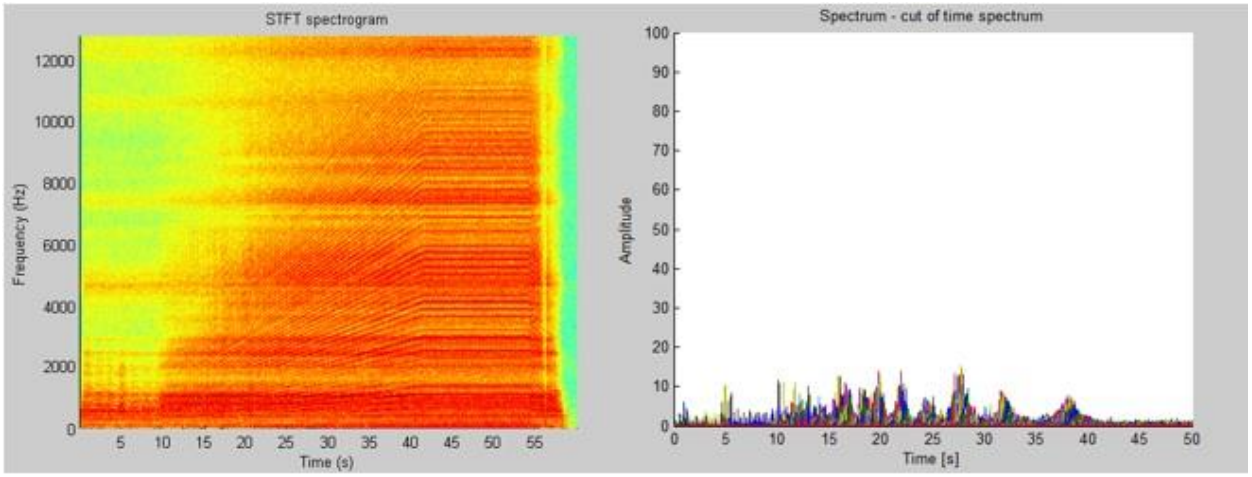

Fig. 4. Spectrogram and projection amplitude-time variant 0 μm

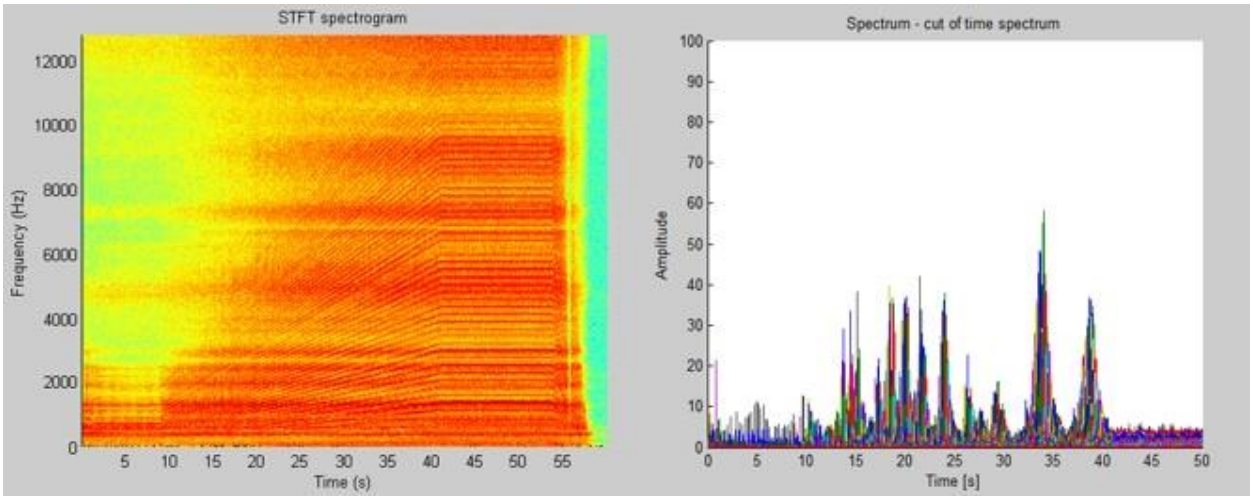

Fig. 5. Spectrogram and projection amplitude-time variant 7.8955 μm

From the previous figures – spectrograms (left side), it is possible to detect a clear difference in the graphical resolution of the spectrograms for each variant of the damage. In the case of a non-damaged bearing, the colour resolution is one-sided, which means that the bearing is in a trouble-free condition. In the case of damaged bearings, it is obvious that with the increase of the deformation degree, the graphical contrast of the individual invariants in the given spectrograms increases. From this finding, it can be said that in the region at 2000 Hz and in period <35, 55 s> (a graphically significant part of the output), there is an increase of amplitude, own oscillations, possible resonance phenomenon and increased noise levels with the given bearing.

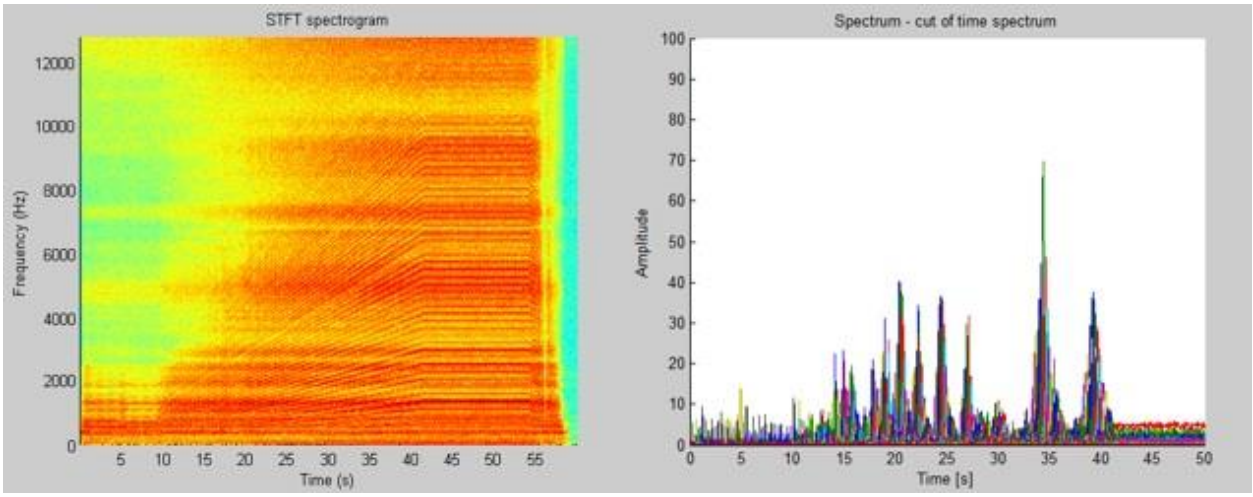

Fig. 6. Spectrogram and projection amplitude-time variant 48.7087 μm

From the time-amplitude projections, it is possible to see that increasing of the amplitude value depends on the deformation on raceways. In case of non-damaged (0 μm), bearing is maximum amplitude value 15 m/s^2, ball bearing with deformation 7.8955 μm shows amplitude 60 m/s^2 and in case of variant with deformation 48.7087 μm is detected amplitude value 70 m/s^2. It means that higher deformation on raceways caused higher values of vibration amplitude.

Evidence of the above findings is also the individual graphical outputs of the spectrogram projections into the time domain where it is possible to detect an increase in the amplitude value depending on the depth of deformation of the path of the bearing.

6. TRANSFORMATION OF MEASURED DATA BY FFT

In the next step, an analysis was performed of stationary mode (only constant speed) by means of a fast Fourier transform using the composing of the measured data through the so-envelopes (2^{15} number of samples) to obtain optimal graphical outputs as shown in Fig. 7-9.

From previous graphical outputs based on fast Fourier transform, which displayed dependence of sampling frequency and amplitude values, it is clear to detect the significant increasing of amplitude values depending on the depth of deformation of the orbital path of the investigated bearings.

Mentioned figures displayed the dependence of vibration amplitudes on deformation. In case of non-damaged (0 μm) bearing is maximum amplitude value 0.8×10^4 m/s^2, ball bearing with deformation 7.8955 μm shows amplitude 1.5×10^5 m/s^2 and in case of variant with deformation 48.7087 μm is detected amplitude value 2×10^5 m/s^2. It means that higher deformation on raceways caused higher values of vibration amplitude therein higher appearance of resonance and higher level of noise.

Based on this finding, it is possible to conclude with certainty that the methodology and the results obtained are correct, as evidenced by the two variants of the algorithms of mathematical methods.

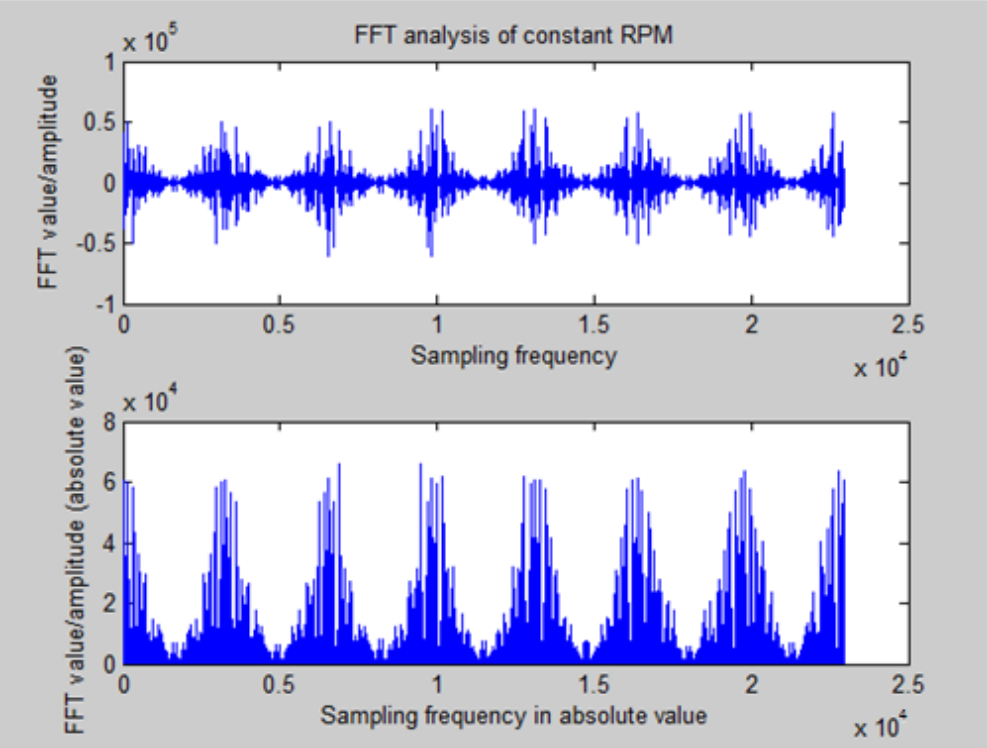

Fig. 7. FFT spectrum variant 0 µm

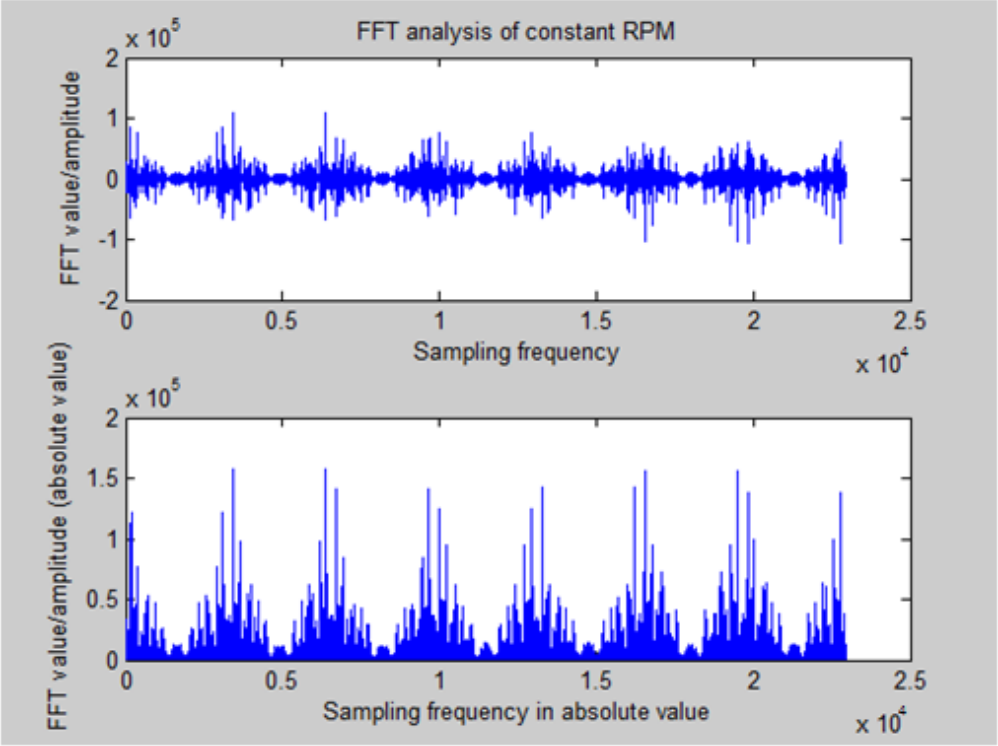

Fig. 8. FFT spectrum variant 7.8955 µm

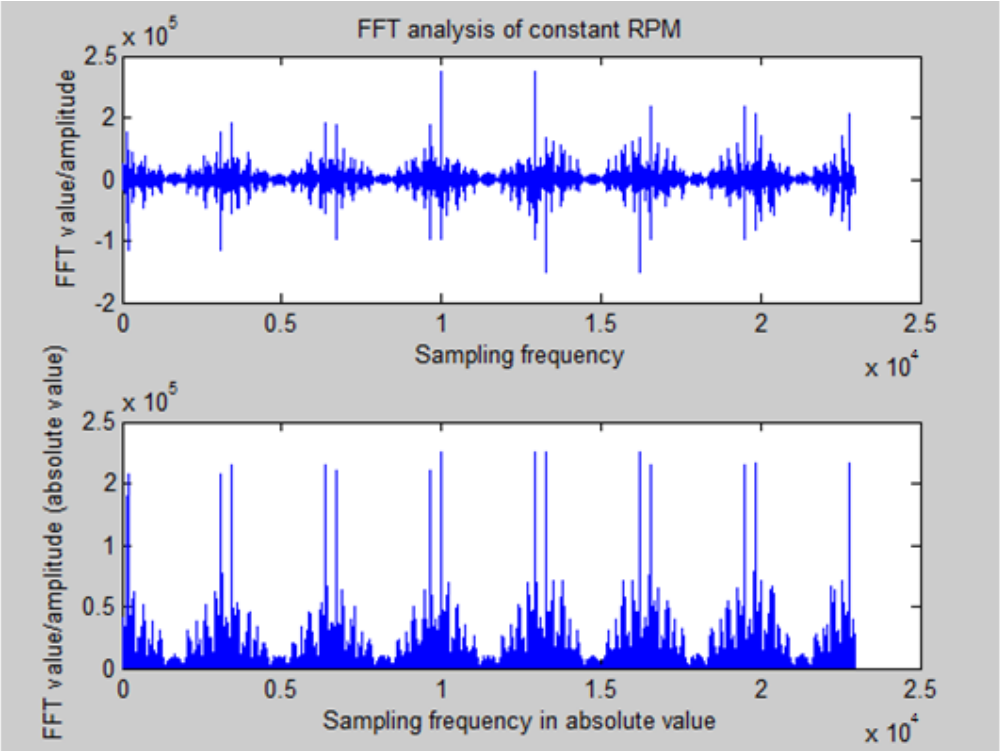

Fig. 9. FFT spectrum variant 48.7087 μm

7. TRANSFORMATION OF MEASURED DATA BY WT

In this section, Wavelet transform analysis was performed with the same objective as the Fourier transform. The aim was to perform and compile individual computational algorithms and compare the results achieved with the purpose of confirming previous findings and to ensure the correctness of selected procedures and methodologies. In the following graphical representations in Fig. 10-12, it is possible to see the individual spectra processed from the measurement results of the three types of bearings with the corresponding deformations on raceways.

From the previous Figs. 10,11, and 12, it can be assumed that in the region at 2000 Hz and in time scale <35, 55 s> (a graphically significant part of the output) there is an increase of amplitude, own oscillations, possible resonance phenomenon and increased noise levels, it relates to the damaged bearings Figs. 11 and 12. Non-damaged bearing Fig. 10 does not show any significant parts in projection, which means no defects and loss of reliability.

In summary of WT, increasing amplitude values in the form of contrast-bright invariants emerging in the z-direction are obvious and clearly visible from Figs. 11 and 12 and non-damaged ball bearing does not show any contrast bright-invariants. These results which confirm the previous results with high accuracy are comparable almost identical to those achieved through STFT and/or FFT computational algorithms.

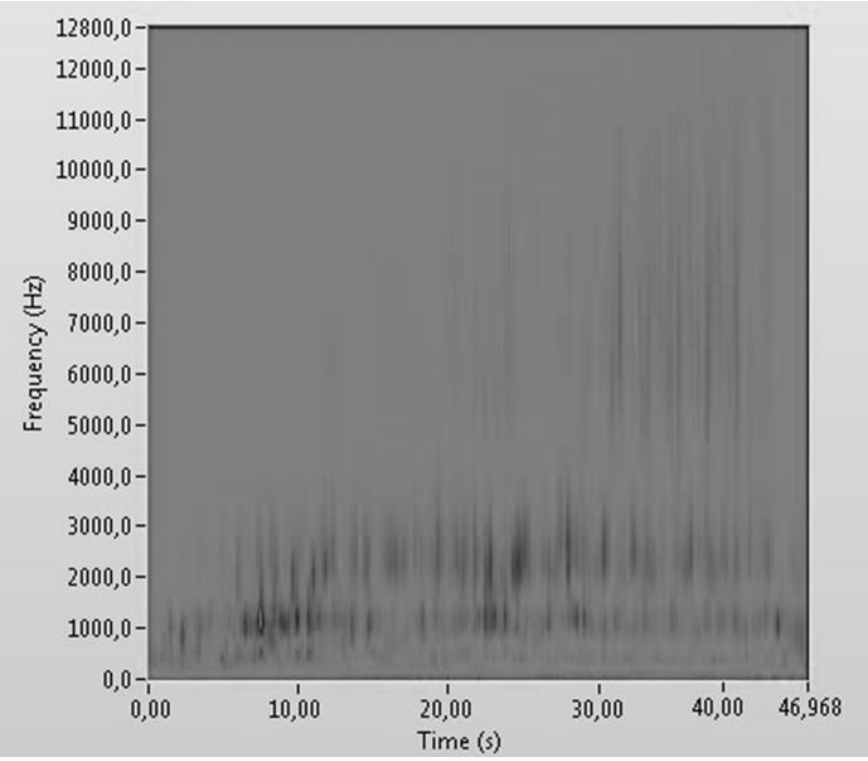

Fig. 10. WT spectrum of ball bearing variant 0 μm

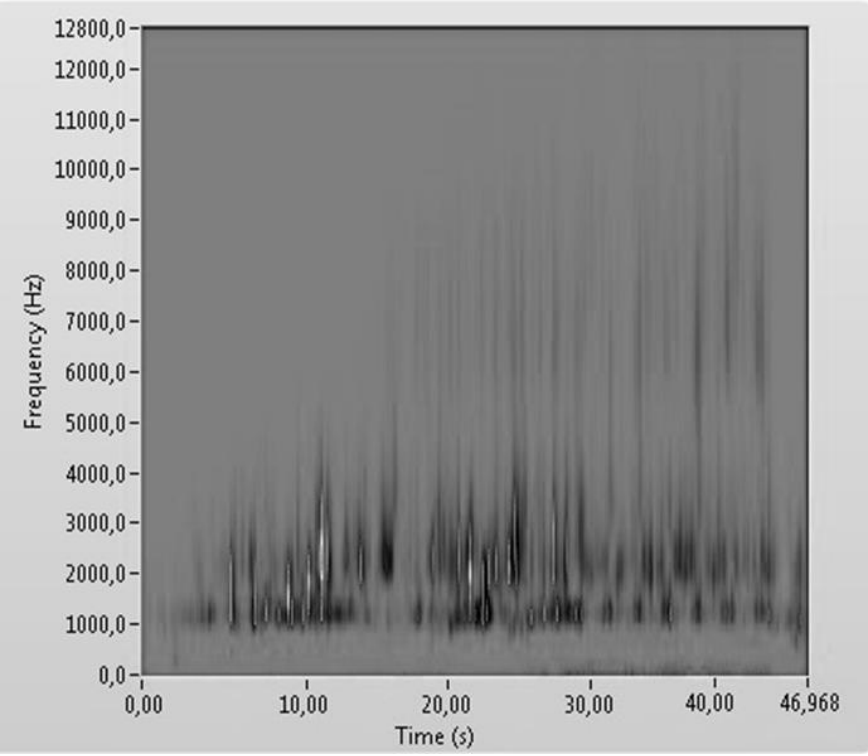

Fig. 11. WT spectrum of ball bearing variant 7.8955 μm

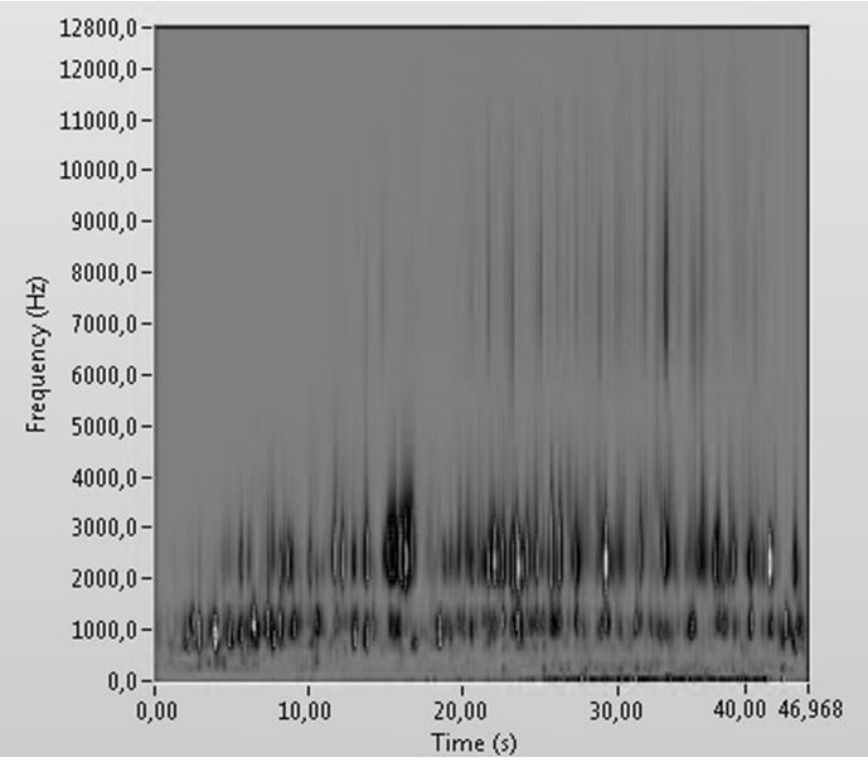

Fig. 12. WT spectrum of ball bearing variant 48.7087 μm

8. LIFETIME PREDICTION THROUGH CALIBRATION DIAGRAMS

Calibration diagrams were generated based on the processing of the measured data in terms of RMS evaluation (effective signal value) through computational models and algorithms. In this simulation, 11 bearings, 10 bearings with individual notches created by experimental loading equipment and 1 undamaged bearing were analysed as shown in Tab. 1. Using the analysis, the dependence of RMS on the impression depth in μm was created. Calibration plots were generated in individual measurement directions (axial, radial, and tangential) corresponding to the radial load cycle during the experiment and shown in Fig. 13-15.

Tab. 1

Individual bearings variants with corresponding deformations on raceways

1. variant	0 μm
2. variant	7,8955 μm
3. variant	8,1881 μm
4. variant	8,5763 μm
5. variant	13,7826 μm
6. variant	14,1388 μm
7. variant	16,7959 μm
8. variant	18,6022 μm
9. variant	40,4592 μm

10. variant	48,2372 μm
11. variant	48,7087 μm

Thus, the calibration charts shown are suggestions for a possible bearing prediction in the presence of orbital deformations. The prediction is based on the principle of the dependence of the indentation depth on the value of the effective signal. The graphs clearly show that when comparing the RMS of the undamaged and damaged bearing (7.8955 μm), a significant increase in the effective value of the signal, which was confirmed in all directions of measurement, occurs.

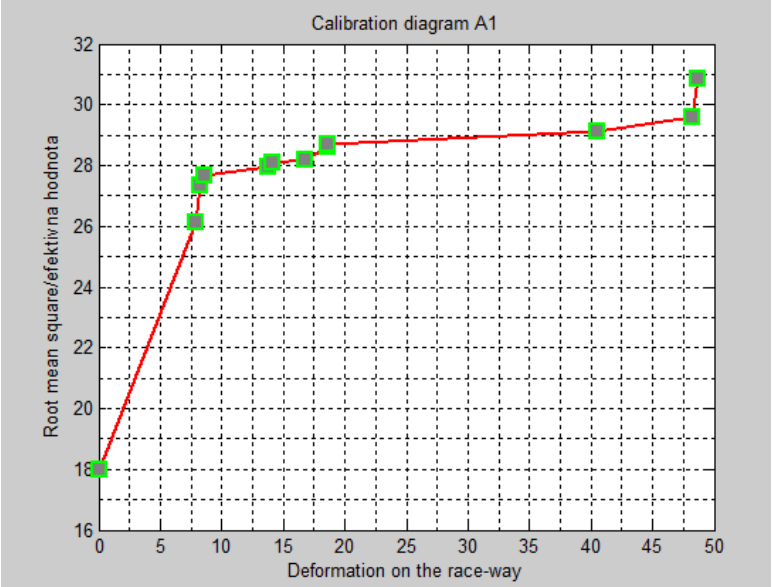

Fig. 13. Calibration diagram of RMS and deformation in the axial direction

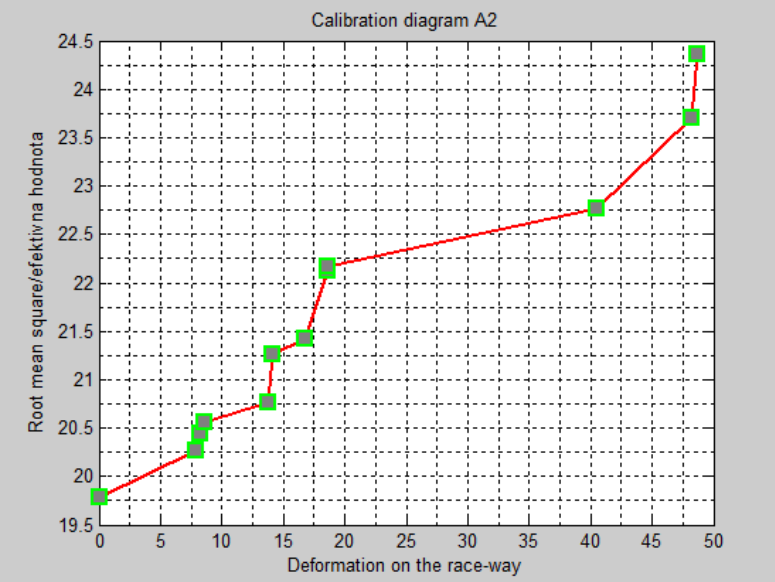

Fig. 14. Calibration diagram of RMS and deformation in the radial direction

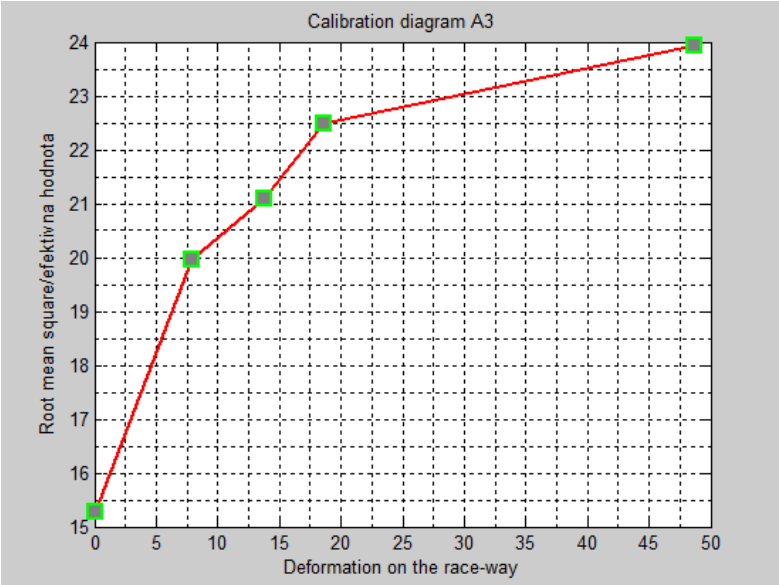

Fig. 15. Calibration diagram of RMS and deformation in the tangential direction

9. CONCLUSION

Measurement, processing and analysis of signals obtained from real machine tool measurements, roller bearings in our case, is an integral part of a comprehensive diagnostic system to monitor operating conditions. The purpose of vibration analysis of machines and their components is to determine the occurrence and causes of oscillation and the consequent possibility of eliminating their occurrence in order to ensure life expectancy and to maximise the reliability of the machine in operation. In our contribution, we discussed the problems of rolling bearings diagnostics, measurement and solution methodology using algorithms based on mathematical methods. From the point of view of the analysis and comparison of the bearings with the different variants of the damage, the amplitude sensitivity, the resonance and the gradient of noise from the level of damage were determined by mathematical methods, which is evidence of graphical outputs and obtained the results of the analysis and getting possible methodology to prediction.

Acknowledgement

This paper was supported by KEGA 017ŽU-4/2017 and by the Slovak Research and Development Agency under contract No. APVV–0736–12.

References

1. Bensana T., S. Mekhilef. 2016. “Numerical and experimental analysis of vibratory signals for rolling bearing fault diagnosis”. *Mechanika* 22(3): 217-224. ISSN 1392-1207.

2. Dekýš Vladimír, Peter Kalman, Pavol Hanák, Pavol Novák, Zuzana Stankovičová. 2016. „Determination of vibration sources by using STFT". *Procedia Engineerin*g 177: 496-501. ISSN 1877 7058. DOI: https://doi.org/10.1016/j.proeng.2017.02.251.
3. Figlus T., M. Stańczyk. 2016. "A method for detecting damage to rolling bearings in toothed gears of processing lines". *Metalurgija* 55(1): 75-78.
4. Frankovský, P., D. Hroncová, I. Delyová, P. Hudák. 2012. „Inverse and forward dynamic analysis of two link manipulator". *Proceedia Engineering* 48: 158-163.
5. Homišin Jaroslav, Robert Grega, Peter Kaššay, Gabriel Fedorko, Vieroslav Molnár. 2019 „Removal of systematic failure of belt conveyor drive by reducing vibrations". *Engineering Failure Analysis* 99: 192-202. ISSN 1350-6307.
6. Kosicka E., Kozłowski E., Mazurkiewicz D. 2015. „The use of stationary tests for analysis of monitored residual processes". *Eksploatacja i Niezawodnosc – Maintenance and Reliability* 17(4): 604–609. DOI: http://dx.doi.org/10.17531/ein.2015.4.17.
7. Močilan Martin, Milan Žmindák, Peter Pastorek, 2016. „Dynamic analysis of fuel tank". *Proceedia Engineering* 136: 45-49. ISSN 1877-7058. 20th International conference machine modeling and simulations "MMS 2015". Terchova, Slovakia.
8. Sága Milan, Róbert Bednár, Milan Vaško. 2011. „Contribution to Modal and Spectral Interval Finite Element Analysis". *Vibration Problems ICOVP 2011 Springer Proceedings in Physics* 139: 269-274. Edited by Jiří Náprstek, Jaromír Horáček, Miloslav Okrouhlík, Bohdana Marvalová, Ferdinand Verhulst, Jerzy T. Sawicki. Springer, Dordrecht. ISBN 978-94-007-2069-5. DOI : https://doi.org/10.1007/978-94-007-2069-5_37.
9. Sága Milan, Peter Kopas, Milan Uhričík. 2012. „Modeling and experimental analysis of the aluminium alloy fatigue damage in the case of bending - torsion loading". *Procedia Engineering* 48: 599-606. ISSN 1877-7058. DOI: https://doi.org/10.1016/j.proeng.2012.09.559.
10. Urbanský Matej, Jaroslav Homišin, Peter Kaššay, Jozef Krajňák. 2018. „Measurement of air springs volume using indirect method in the design of selected pneumatic devices". *Acta Mechanica et Automatica* 12(1): 19-22. ISSN 1898-4088.
11. Vavro Ján jr., Ján Vavro, Petra Kováčiková, Radka Bezdedová. 2016. „Kinematic and dynamic analysis of the manipulator for removal of rough tyres". *Proceedia Engineering* 136: 120-124. ISSN 1877-7058. DOI: 10.1016/j.proeng.2016.01.184. 20th International conference machine modelling and simulations "MMS 2015". Terchova, Slovakia.
12. Zieja Mariusz, Paweł Gołda, Mariusz Żokowski, Paweł Majewski. 2017. „Vibroacoustic technique for the fault diagnosis in a gear transmission of a military helicopter". *Journal of Vibroengineering* 19(2): 1039-1049.

Received 18.10.2019; accepted in revised form 22.12.2019